Synthetic Analogues for Oxovanadium(IV) – Glutathione Interaction: An EPR, Synthetic and Structural Study of Oxovanadium(IV) Compounds with Sulfhydryl-Containing Pseudopeptides and Dipeptides

Anastasios J. Tasiopoulos,[a] Anastasios N. Troganis,[c] Angelos Evangelou,[d] Catherine P. Raptopoulou,[b] Aris Terzis,[b] Yiannis Deligiannakis,*[b] and Themistoklis A. Kabanos*[a]

Abstract: Valuable analogues of the $V^{IV}O^{2+}$ – glutathione complex have been synthesized and characterized. The reaction of $[V^{IV}O(CH_3COO)_2(phen)]$ (phen = 1,10-phenanthroline) with the sulfhydryl-containing pseudopeptides (scp) *N*-(2-mercaptopropionyl)cysteine (H_4m_2pc), and *N*-(3-mercaptopropionyl)cysteine (H_4m_3pc) in the presence of triethylamine gives the oxovanadium(IV) compounds $[(Et_3NH)_2][VO(m_2pc)]$ (**1**) and $[(Et_3NH)_2][VO(m_3pc)]$ (**2**), while reaction of $[VOCl_2(phen)]$ with the scp *N*-(2-mercaptopropionyl)glycine (H_3mpg) and the dipeptides glycylglycine ($H_2glygly$) and glycyl-L-alanine ($H_2glyala$) in the presence of triethylamine results in the formation of the compounds $[Et_3NH][VO(mpg)(phen)]$ (**3**), $[VO(glygly)(phen)]\cdot 2CH_3OH$ (**4**$\cdot 2CH_3OH$), and $[VO(glyala)(phen)]\cdot CH_3OH$ (**5**$\cdot CH_3OH$). Complex $[VOCl_2(phen)(CH_3OH)]$ (**7**) was prepared by the reaction of $[VOCl_2(thf)_2]$ with phen in a methanolic solution. The X-ray structure of **3** shows that the vanadium(IV) atom is ligated to a tridentate mpg^{3-} ligand at the $S_{thiolato}$, $N_{peptide}$ and $O_{carboxylato}$ atoms. The X-ray structure of **7** is also reported. The optical, infrared, magnetic, electron paramagnetic resonance, and electrochemical properties of compounds **1**–**5**$\cdot CH_3OH$ and **7** were studied. Combination of the correlation plots of the EPR parameters g_z versus A_z, or the ground-state orbital population $(\beta^*)^2$ versus A_z, together with the additivity relationship, $A_{z,calcd} = \Sigma n_i A_{zi}/4$, were shown to provide a powerful tool for probing the equatorial donor atoms in an oxovanadium(IV) compound and consequently in biomolecules. Thus, these methods provide valuable evidence for the assignment of the equatorial donor atoms for the $V^{IV}O^{2+}$ center of the $V^{IV}O^{2+}$ – glutathione system at various pH values. Model NMR studies (interaction of vanadium(V) with H_3mpg) showed that there is a possibility of vanadium(V) ligation to glutathione. The contribution of a deprotonated peptide(amide) nitrogen to A_z is not a fixed quantity (it varies from 29 to 43×10^{-4} cm^{-1}), but is influenced by the presence of the three other donor atoms in the equatorial plane and, in particular, their charge.

Keywords: glutathione • pseudopeptides • S ligands • solid-state structures • vanadium

[a] Dr. T. A. Kabanos, A. J. Tasiopoulos
Department of Chemistry, Section of Inorganic and Analytical Chemistry
University of Ioannina, GR-45110 Ioannina (Greece)
Fax: (+30) 651-44831
E-mail: tkampano@cc.uoi.gr

[b] Dr. Y. Deligiannakis, Dr. C. P. Raptopoulou, Prof. A. Terzis
NRCPS Demokritos, Institute of Materials Science
GR-15310 Agia Paraskevi Attikis (Greece)
Fax: (+30) 1-6519430
E-mail: deli@ims.demokritos.t.gr

[c] Dr. A. Troganis
Department of Chemistry, NMR Center, University of Ioannina
GR-45110 Ioannina (Greece)

[d] Dr. A. Evangelou, M.D.
Laboratory of Experimental Physiology, Faculty of Medicine
University of Ioannina, GR-46110 Ioannina (Greece)
Fax: (+30) 651-67874

Supporting information for this article is available on the WWW under http://www.wiley-vch.de/home/chemistry/ or from the author.

Introduction

Vanadium is an essential nutrient for higher animals,[1] although this has not yet been clearly proved for humans.[2] Nevertheless, vanadium generates significant physiological responses in vivo;[3] for example, vanadate inhibits ion-transport ATPases,[4] phosphotyrosine phosphatase,[5] and so forth. Vanadium has also proved effective in treatment of experimentally induced cancers in Wistar rats,[6] but indisputably the most important physiological effect of vanadium is the stimulation of glucose uptake and glucose metabolism, that is, its insulin-like properties.[7] Diabetes is one of many diseases which have been reported to have an oxidative pathology.[8] Glutathione, the cysteine-containing tripeptide (γ-glutamylcysteinylglycine), which is found in millimolar concentrations in all animal cells, provides the principal intracellular defense against oxidative stress[9] and participates in detoxification of many foreign molecules.[10] Gluta-

0947-6539/99/0503-0910 $ 17.50+.50/0

thione depletion results in hepatic and renal failure and ultimately in death. In vitro studies have shown that depression of intracellular glutathione levels decreases cell survival,[11] alters T-cell functions,[12] and increases HIV replication,[13, 14] NF-*k*B activation[13, 14] and sensitivity to tumor-necrosis-factor-induced cell death.[15] Clinical studies directly link glutathione deficiency to impaired survival in HIV disease.[16]

Various studies have shown that glutathione plays an important role in relation to the biochemistry of vanadium.[17] Inside the red blood cells vanadium(V) is reduced to $V^{IV}O^{2+}$ by glutathione,[18–24] which can also act as a ligand for the generated oxovanadium(IV) cation.[25–29] Unfortunately, no crystallographic information is available for any $V^{IV}O^{2+}$–glutathione species at the present time. There are only a few solution studies concerning the interaction of $V^{IV}O^{2+}$ with glutathione,[25–29] but there is controversy about the ligating groups of glutathione to vanadium.[25–29] Since sulfhydryl-containing peptides (or pseudopeptides) provide ideal molecules for the synthesis of analogues of the oxovanadium(IV)–glutathione compounds, we embarked on the synthesis of the oxovanadium(IV) compounds with the sulfhydryl-containing pseudopeptides *N*-(2-mercaptopropionyl)glycine (H_3mpg), *N*-(2-mercaptopropionyl)cysteine (H_4m_2pc), and *N*-(3-mercaptopropionyl)cysteine (H_4m_3pc) (Scheme 1). Similarities between the constitution of H_3mpg and the right-hand portion of glutathione (GSH) and between the constitution of H_4m_2pc and H_4m_3pc and the middle portion of glutathione (Scheme 1) were one clear reason for our choice. Herein, we describe the synthesis of oxovanadium(IV) species with the sulfhydryl-containing pseudopeptides H_3mpg, H_4m_2pc, H_4m_3pc, as well as with the dipeptides glycylglycine and glycylalanine. The X-ray crystal structure of the [VO(mpg)(phen)]$^-$ anion is also reported. In addition, the optical, infrared, magnetic, electron paramagnetic resonance (EPR), and electrochemical properties of the oxovanadium(IV) compounds and NMR (^{1}H, ^{13}C, ^{51}V) studies of the reaction of vanadium(V) with the sulfhydryl-containing pseudopeptide H_3mpg are reported. A preliminary report of this research has been communicated previously.[30]

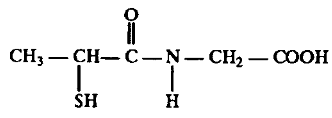

H_3mpg

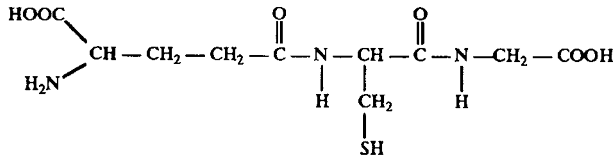

GSH

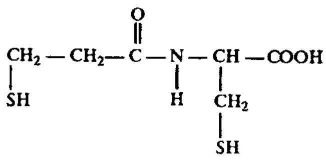

H_4m_3pc

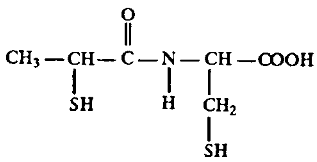

H_4m_2pc

Scheme 1. Glutathione (GSH) compared with sulfhydryl-containing pseudopeptides *N*-(2-mercaptopropionyl)glycine (H_3mpg), *N*-(2-mercaptopropionyl)cysteine (H_4m_2pc), and *N*-(3-mercaptopropionyl)cysteine (H_4m_3pc).

Abstract in Greek: Η αντίδραση του [$V^{IV}O(CH_3COO)_2$(phen)] {phen=1,10-φαινανθρολίνη} με τα σουλφιδρυλικά ψευδοπεπτίδια (**σψ**), *N*-(2-μερκάπτοπροπιονύλ)κυστεΐνη (H_4m_2pc) και *N*-(3-μερκάπτοπροπιονύλ)κυστεΐνη (H_4m_3pc), παρουσία τριαιθυλαμίνης, οδηγεί στο σχηματισμό των ενώσεων $(Et_3NH)_2[VO(m_2pc)]$ (**1**) και $(Et_3NH)_2[VO(m_3pc)]$ (**2**), ενώ η αντίδραση του [$VOCl_2$(phen)] με το **σψ** *N*-(2-μεκράπτοπροπιονύλ)γλυκίνη (H_3mpg) και τα διπεπτίδια γλυκυλογλυκίνη (H_2glygly) και γλύκυλο-L-αλανίνη (H_2glyala), παρουσία τριαιθυλαμίνης, έχει ως αποτέλεσμα το σχηματισμό των ενώσεων Et_3NH[VO(mpg)(phen)] (**3**), [VO(glygly)(phen)]·2CH_3OH (**4**·2CH_3OH) και [VO(glyala)(phen)]·CH_3OH (**5**·CH_3OH). Το σύμπλοκο [$VOCl_2$(phen)(CH_3OH)] (**7**) παρασκευάστηκε με την αντίδραση του [$VOCl_2(thf)_2$] με phen σε διάλυμα μεθανόλης. Οι κρυσταλλικές δομές των ενώσεων **3** και **7** έχουν επιλυθεί και αναφέρονται. Τα φάσματα ορατού-υπεριώδους, υπερύθρου, ηλεκτρονικού παραμαγνητικού συντονισμού (EPR), καθώς επίσης οι μαγνητικές και ηλεκτροχημικές ιδιότητες των ενώσεων **1**-**5**·CH_3OH και **7** μελετήθηκαν. Συνδυασμός των διαγραμμάτων συσχέτισης των παραμέτρων EPR g_z συναρτήσει A_z, ή της πιθανότητας κατάληψης της θεμελιώδους κατάστασης $(\beta^*)^2$ συναρτήσει A_z, με την προσθετική σχέση $A_{z,calc}=\sum n_i A_{zi}/4$, αποτελεί ένα ισχυρό εργαλείο για την πρόβλεψη των ατόμων δοτών στο ισημερινό επίπεδο μιας απλής ένωσης του οξοβαναδίου(IV) και συνεπώς στα βιομόρια. Ετσι, για το σύστημα $V^{IV}O^{2+}$-γλουταθειόνης που μελετήθηκε, αυτός ο συνδυασμός βοήθησε την πρόβλεψη των ατόμων δοτών στο ισημερινό επίπεδο. Πρότυπες [αντίδραση του βαναδίου(V) με το H_3mpg] μελέτες NMR έδειξαν ότι υπάρχει πιθανότητα ένταξης της γλουταθειόνης με το βανάδιο(V). Η συνεισφορά ενός αποπρωτονιωμένου πεπτιδικού (αμιδικού) αζώτου στην συνολική τιμή A_z (βασισμένη στην προσθετική σχέση) δεν είναι μια καθορισμένη ποσότητα (ποικίλλει από 29 μέχρι 43 x 10^{-4} cm^{-1}), αλλά επηρεάζεται από την παρουσία των τριών άλλων ατόμων δοτών στο ισημερινό επίπεδο και ειδικά από το φορτίο τους.

Results and Discussion

Synthesis of the compounds: Compound **3** was prepared by sequential treatment of [$VOCl_2(thf)_2$] with 1,10-phenanthroline, H_3mpg and excess triethylamine [Eqs. (1) and (2)] inacetonitrile, after a few modifica-

$$[VOCl_2(thf)_2] + phen \rightarrow [VOCl_2(phen)] + 2\,thf \quad (1)$$

$$[VOCl_2(phen)] + H_3mpg + 3\,Et_3N \rightarrow \underset{\mathbf{3}}{[Et_3NH][VO(mpg)(phen)]} + 2\,Et_3NHCl \quad (2)$$

tions of the original procedure.[30] By the same protocol, **1** and **2** were successfully prepared as mixtures with Et_3NHCl [Eq. (2)]. Because the solubilities of **1**, **2**, and Et_3NHCl were almost identical in various organic solvents, **1** and **2** could not be separated from Et_3NHCl. This required the development of an alternative method for the synthesis of pure **1** and **2**.

When $[VO(CH_3COO)_2]$ was refluxed with 1,10-phenanthroline in acetonitrile, $[VO(CH_3COO)_2(phen)]$ was formed, which is slightly soluble in acetonitrile. Addition of the sulfhydryl-containing pseudopeptide (H_4m_2pc or H_4m_3pc) and excess of triethylamine resulted in the formation of the desired products [Eq. (3)]. Evaporation of the solution

$$[VO(CH_3COO)_2(phen)] + H_4m_2pc + 4Et_3N \rightarrow [(Et_3NH)_2][VO(m_2pc)] + phen + 2\,Et_3NH^+CH_3COO^- \quad (3)$$
$$\mathbf{1}$$

to dryness gave a mixture of **1** or **2**, 1,10-phenanthroline, and $Et_3NH^+CH_3COO^-$, and since the by-products are soluble in toluene, while **1** and **2** are insoluble; trituration of the mixture with toluene gives pure **1** and **2**.

We also prepared compound **3** by substituting $[VO(acac)_2]$ for $[VOCl_2(thf)_2]$ (method 3B). The only disadvantage of this method is the duration of the preparation (2 h for method 3A; ≈12 h for method 3B).

The oxovanadium(IV) compounds with the dipeptides H_2glygly(**4**·2CH_3OH, [VO(glygly)(phen)]·2CH_3OH) and H_2glyala (**5**·CH_3OH, [VO(glyala)(phen)]·CH_3OH) were prepared following procedure 3A, while compounds **6** ($[(Et_4N)_2][VOCl_4]$) and **7** ($[VOCl_2(phen)(CH_3OH)]$) were prepared by treating $[VOCl_2(thf)_2]$ with two equivalents of Et_4NCl (in CH_2Cl_2) and one equivalent of phen (in CH_3OH), respectively.

Compounds **1** to **5**·CH_3OH, in the solid state, are stable under inert atmosphere at approximately −20 °C for only about two weeks. In solution, under argon and at ambient temperature (35–40 °C), they are stable for only ≈1 min or even less, while at around −15 °C they are stable for at least 10 min.

Crystallography: A selection of interatomic distances and bond angles relevant to the vanadium coordination sphere for compound **3**·CH_3OH are listed in Table 1. The molecular structure of the anion of **3**, illustrated in Figure 1, shows the vanadium atom possessing a severely distorted octahedral coordination; as far as we are aware, this is the first structure reported in which the mpg^{3-} ion is ligated to a metal ion as a nonbridging chelating ligand. The only other structural study with mpg^{3-} was one of the cyclic trimeric nickel(II) complex $[Ni_3(mpg)_3]^{3-}$, in which mpg^{3-} acts as a bridging (through the thiolato sulfur) chelating ligand.[31] The vanadium atom in **3**·CH_3OH is bonded to a tridentate mpg^{3-} ligand at the $S_{thiolato}$ atom, the deprotonated $N_{peptide}$ atom N(1), and one of the $O_{carboxylato}$ atoms O(2), as well as an oxo group O(1) and two phenanthroline nitrogens N(2) and N(3), and is 0.36 Å above the mean equatorial plane (mean deviation 0.015 Å), defined by the three ligating atoms of the pseudodipeptide mpg^{3-} [S, N(1), and O(2)] and a phenanthroline nitrogen N(2), in the direction of the oxo ligand. The peptide functionality C(1)–C(2)–O(4)–N(1) is planar within the limits of precision. The ligand mpg^{3-} forms two five-membered fused chelate rings and is meridionally ligated to the $V^{IV}O^{2+}$ center with the thiolato sulfur and the carboxylato oxygen atoms lying in a *trans* position. The $V{-}N_{peptide}$ bond length [1.997(4) Å] is almost identical to the reported mean $V{-}N_{amide}$ value[32] [1.999(12) Å] for various vanadium–aromatic amide structures, but it is substantially longer (≈0.07 Å) than the $V{-}N_{peptide}$ bond length of the only other oxovanadium(IV)–peptide compound structurally characterized,[33] [VO(glytyr)(phen)] [$V{-}N_{peptide}$ = 1.927(7) Å]. At this point, it is worth mentioning that the mean $d(V^{IV}{-}N_{amido})$ (where N_{amido} is the nitrogen of the R_2N^- functionality) is ≈1.90 Å.[34] The V−S,[32, 35–40] V=O(1),[41] and V−O(2)[42] bond lengths [2.3820(14), 1.602(3) and 2.014(4) Å, respectively] are consistent with values found in other oxovanadium(IV) compounds. The 1,10-phenanthroline is unsymmetrically ligated to vanadium, with a long V−N(3) bond [2.343(4) Å] oriented *trans* to the oxo ligand and a short V−N(2) bond [2.173(4) Å] in the equatorial plane oriented *trans* to the deprotonated amide nitrogen. The V−N(3) bond length is consistent with the literature values,[41, 43] while the strong *trans* influence of the deprotonated amide nitrogen [N(1)] gives rise to a rather long V−N(2) bond compared to the literature values for bpy compounds, observed in the range 2.10–2.15 Å.[42–46]

Figure 2 shows a perspective view of **7**. The vanadium is in a distorted octahedral environment consisting of two phenanthroline nitrogens, two *cis*-chlorines, a methanolic oxygen and an oxo group and is 0.31 Å above the mean equatorial plane

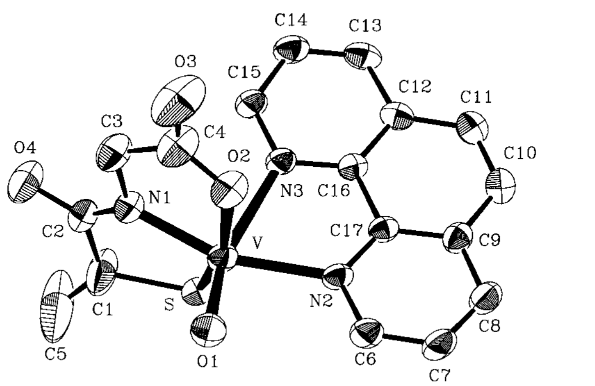

Figure 1. Structure of the anion of **3** showing thermal ellipsoids at 50% probability and the atom numbering scheme. For clarity hydrogen atoms are omitted.

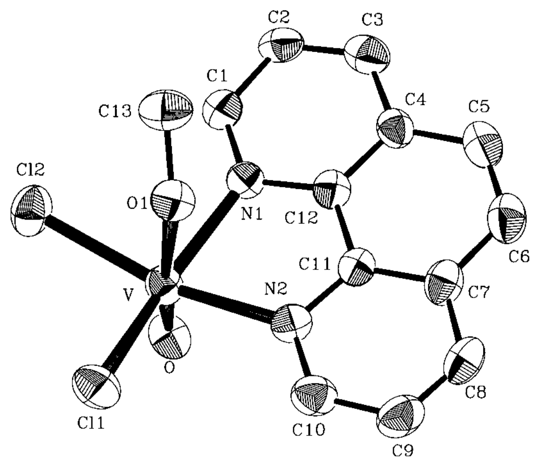

Figure 2. Structure of **7** showing thermal ellipsoids at 50% probability and the atom numbering scheme. For clarity hydrogen atoms are omitted.

  0947-6539/99/0503-0912 $ 17.50+.50/0 *Chem. Eur. J.* **1999**, *5*, No. 3

Table 1. Interatomic distances (Å) and angles (°) relevant to the vanadium coordination sphere for complex $3 \cdot CH_3OH$.

Bond lengths [Å]			
V–O(1)	1.602(3)	V–N(2)	2.173(4)
V–O(2)	2.014(4)	V–N(3)	2.343(4)
V–N(1)	1.997(4)	V–S	2.3820(14)
Bond angles [°]			
O(1)-V-N(1)	108.9(2)	O(2)-V-N(3)	78.73(14)
O(1)-V-O(2)	100.4(2)	N(2)-V-N(3)	71.81(12)
N(1)-V-O(2)	79.9(2)	O(1)-V-S	101.8(2)
O(1)-V-N(2)	90.3(2)	N(1)-V-S	81.74(12)
N(1)-V-N(2)	160.2(2)	O(2)-V-S	154.81(11)
O(2)-V-N(2)	92.15(14)	N(2)-V-S	99.46(10)
O(1)-V-N(3)	162.0(2)	N(3)-V-S	83.75(9)
N(1)-V-N(3)	88.8(2)		

(mean deviation 0.015 Å), defined by the two phenanthroline and the two chlorine atoms, in the direction of the oxo ligand. A strong *trans* influence observed in most oxovanadium(IV) species suggests that the weakest donor atom should be *trans* to the oxo group. This expectation is fulfilled in complex **7**, which adopts the predicted structure with a long V–O(1) bond [2.301(4) Å] (Table 2) oriented *trans* to the oxo ligand. The

Table 2. Interatomic distances and angles relevant to the vanadium(IV) coordination shpere for **7**.

Bond lengths [Å]			
V–O	1.626(3)	V–O(1)	2.301(4)
V–N(2)	2.148(4)	V–Cl(1)	2.327(2)
V–N(1)	2.153(4)	V–Cl(2)	2.365(2)
Bond angles [°]			
O-V-N(2)	95.6(2)	N(1)-V-Cl(1)	161.04(10)
O-V-N(1)	95.0(2)	O(1)-V-Cl(1)	86.52(10)
N(2)-V-N(1)	77.60(14)	O-V-Cl(2)	99.16(13)
O-V-O(1)	171.42(14)	N(2)-V-Cl(2)	163.75(11)
N(2)-V-O(1)	81.31(14)	N(1)-V-Vl(2)	94.27(11)
N(1)-V-O(1)	76.58(13)	O(1)-V-Cl(2)	83.12(11)
O-V-Cl(1)	101.61(12)	Cl(1)-V-Cl(2)	92.14(7)
N(2)-V-Cl(1)	91.56(11)		

V–Cl bond lengths [V–Cl(1) 2.327(2) and V–Cl(2) 2.365(2) Å] and the V=O bond length [1.626(3) Å] are consistent with V–Cl and V=O bond lengths found in mononuclear octahedral vanadium compounds containing the *cis*-V^{IV}OCl unit,[47] V–Cl(2) being longer than V–Cl(1) [≈0.04 Å] as a result of its involvement in the hydrogen bond: H[O(1)]···Cl(2) = 3.076(4) Å, H[O(1)]–O(1) = 0.708 Å, H[O(1)]···Cl(2) = 2.38(5) Å, O(1)-H[O(1)]-Cl(2) = 169(5)°. The 1,10-phenanthroline is symmetrically ligated to vanadium, and the two V–N(1,2) bond lengths are almost equal [≈2.15 Å] and correspond to the higher limit of V–N equatorial bond lengths reported in the literature for similar ligands.[42–46]

Electronic spectra: Table 3 lists the spectral data for the oxovanadium(IV) compounds **1**–**7**. The solution spectra of **1** to **5**·CH_3OH in ethanol and methanol (compounds **3**–**5**·CH_3OH) display two visible bands (or shoulders) at 720–680 and 495–450 nm. The lower energy, low-intensity (ε = 47–76 $M^{-1}cm^{-1}$) band (or shoulder) is assigned[48] as the $b_2(d_{xy}) \rightarrow e(d_{xz},d_{yz})$ transition, assuming C_{4v} symmetry for these compounds. The intensity of the shorter-wavelength band (ε = 530–790 $M^{-1}cm^{-1}$) is high for a spin-forbidden d–d transition and rather low for a charge-transfer transition. We assign[48] this band to the $b_2(d_{xy}) \rightarrow b_1(d_{x^2-y^2})$ transition under C_{4v} symmetry. The spectra also exhibit a third band in the ultraviolet region (359–348 nm, ε = 1020–1520 $M^{-1}cm^{-1}$) which can be assigned as ligand–metal charge transfer; this band probably obscures the expected[48] third [$b_2(d_{xy}) \rightarrow a_1(d_{z^2})$] d–d transition. When dichloromethane or acetonitrile are used as solvents, the situation is almost the same as with ethanol except that (1) the band at 720–680 nm is absent from the spectra of **1**, **2**, and **3**, and (2) a shoulder is present in the spectra of **1** and **2** at 460 nm and 485 nm for acetonitrile and dichloromethane, respectively. The spectra of compounds **6** and **7** have a low-intensity band at 763 and 725 nm, which is

Table 3. UV/Visible spectral data for the oxovanadium(IV) compounds **1** to **7**.

Compound	Solvent	λ_{max} (nm) [ε ($M^{-1}cm^{-1}$)]
1	ethanol	680 (sh) (83), 495 (620), 352 (1230), 291 (sh) (7200), 270 (17 000), 227 (26 500), 201 (30 000)
	acetonitrile	[a] 532 (760), 352 (1280), 289 (sh) (8000), 269 (19000), 226 (28000), 200 (34000)
	dichloromethane	[b] 534 (520), 355 (980), 291 (sh) (8900), 271 (21000), 227 (30000)
2	ethanol	680 (sh) (80), 495 (600), 351 (1220), 291 (sh) (7300), 270 (17500), 227 (27000) 201 (30000)
	acetonitrile	[a] 532 (750), 352 (1250), 289 (sh) (8000), 269 (19000), 226 (28500), 200 (34000)
	dichloromethane	[b] 534 (520), 355 (970), 291 (sh) (8900), 271 (21000), 227 (30000)
3	methanol	720 (51), 471 (580), 348 (1380), 292 (sh) (8500), 270 (22200), 226 (32000), 202 (34000)
	ethanol	720 (76), 487 (790), 352 (1520), 290 (sh) (9000), 270 (21500), 227 (32200), 201 (33000)
	acetonitrile	532 (910), 356 (1500), 288 (sh) (9000), 269 (22000), 225 (31000), 200 (35000)
	dichloromethane	510 (810), 356 (1540), 291 (sh) (8900), 271 (20000), 226 (29700)
4·$2CH_3OH$	methanol	712 (52), 446 (530), 356 (1020), 291 (sh) (8700), 271 (24000), 226 (34700), 202 (34200)
	ethanol	704 (71), 450 (630), 358 (1060), 291 (sh) (9800), 272 (24500), 227 (33000), 202 (32500)
	acetonitrile	700 (79), 456 (780), 358 (1080), 291 (sh) (10000), 270 (26000), 226 (34000), 201 (36000)
5·CH_3OH	methanol	707 (47), 447 (610), 357 (1200), 291 (sh) (9600), 271 (25600), 227 (36600), 202 (35000)
	ethanol	701 (66), 452 (700), 359 (1150), 291 (sh) (10600), 272 (27000), 227 (36000), 202 (35000)
	acetonitrile	703 (80), 463 (700), 360 (820), 290 (sh) (9700), 271 (26000), 227 (34500), 201 (35500)
6	methanol	763 (30), 218 (2000), 198 (3000)
7	methanol	725 (35), 417 (sh) (150), 292 (sh) (9000), 274 (25500), 226 (28500), 203 (32000)

[a] Compounds **1** and **2** display a shoulder at 460 nm with an ε value of ≈600 $M^{-1}cm^{-1}$. [b] Compounds **1** and **2** display a shoulder at 485 nm with an ε value of ≈480 $M^{-1}cm^{-1}$.

assigned as the $b_2(d_{xy}) \rightarrow e(d_{xz},d_{yz})$ transition. Complex **7** also displays a shoulder at 417 nm.

Electrochemistry: The results of the cyclic voltammetric and polarographic studies for the complexes **1–5** · CH_3OH are given in Table 4. The polarographic investigations reveal one-

Table 4. Electrochemical data: cyclic voltammetric and polarographic studies of the compounds **1–5** · CH_3OH.[a]

Compound	E_{pc} [V]	E_{pa} [V]	i_{pc}/i_{pa}	ΔEp[b] [mV]	$E_{1/2}$[c] [V]
1	−1.320[d]	−1.260 0.344	1.0	60	−1.290 (−0.91)
2	−1.400[d]	−1.310 0.340	1.0	90	−1.355 (−0.92)
3	−1.466[d]	−1.380 0.191	1.0	86	−1.423 (−1.28)
	−1.485[e]	−1.620 0.144	1.0	232	−1.735 (−1.33)
4 · 2 CH_3OH	−1.303[d]	−1.207 0.870	1.0	96	−1.255 (−0.85)
5 · CH_3OH	−1.291[d]	−1.231 0.900	1.0	60	−1.261 (−0.89)

[a] All potentials are relative to NHE. [b] $\Delta E_p = |E_{pc} - E_{pa}|$ at a scan rate of 100 mV s^{-1}. [c] Values of the redox potentials ($E_{1/2}$) were calculated from the formula $E_{1/2} = 0.5\,(E_{pa} + E_{pc})$ from cyclic voltammmetric measurements, while values in parentheses of the reduction potentials were obtained from the intercepts of plots of $\log[(i_d - i)/i]$ vs. potential (E). [d] In acetonitrile. [e] In dichloromethane.

electron reversible redox process at −0.91, −0.92, −1.28, −0.85, and −0.89 for **1** to **5** · CH_3OH, respectively. Cyclic voltammetric examination shows the presence of one redox couple at negative potentials and an anodic peak at positive potentials for all the compounds. The peak separation ΔE_p for compounds **1** and **5** · CH_3OH is almost identical (60 mV) to that anticipated for a Nernstian one-electron process (59 mV);[49] plots of cp (peak current) versus $SR^{1/2}$ (SR = scan rate) are linear, and the ratio of the cathodic to anodic peak currents is 1.0, indicating that electron transfer is reversible and that mass transfer is limited, while the peak separation for compounds **2**, **3**, and **4** · 2 CH_3OH is 90 mV, indicating quasireversible behavior.

A control cyclic voltammetric run (in acetonitrile) of the molecules phen, H_3mpg, H_4m_2pc, and H_4m_3pc (the dipeptides H_2glygly and H_2glyala are insoluble in acetonitrile) in the potential range −1.6 to 0.0 V reveals no redox activity for phen, while all the other molecules reveal two reduction peaks at approximately −0.4 V and −1.0 V; thus, it is most likely that the reversible one-electron redox processes observed for compounds **1**, **2**, and **3** are metal-centered. The redox potentials for **4** · 2 CH_3OH and **5** · CH_3OH are shifted anodically (≈0.2 V) compared with the redox process of **3**, and this is reasonable, assuming octahedral geometry for **4** · 2 CH_3OH and **5** · CH_3OH (vide infra), since the only difference between them is that an amino group ($-NH_2$) has been substituted for a deprotonated thiol group. Taking this and the fact that ligand-based redox processes are rarely reversible into account, the redox processes for these compounds can be classified as metal-based. The redox process for compound **1** is summarized in Equation (4).

$$[V^{IV}O(m_2pc)]^{2-} \rightleftharpoons [V^{III}O(m_2pc)]^{3-} \qquad E_{1/2} = -1.290\ \mathrm{V} \tag{4}$$

Infrared spectroscopy: In the IR spectra, compounds **4** · 2 CH_3OH, **5** · CH_3OH, and **7** exhibit medium- to high-intensity bands at 3520, 3535, and 3370 cm^{-1}, respectively, assignable to ν(OH).[50] Compounds **4** · 2 CH_3OH and **5** · CH_3OH exhibit a pair of bands at 3345, 3240 and 3240, 3125 cm^{-1}, respectively; the higher frequency band is assigned to the antisymmetric stretching vibration of the $-NH_2$ group,[50] while the lower frequency band is assigned to its symmetric stretching vibration. The ν_{as}(COO) and ν_s(COO)[50] bands are at 1560, 1384 (**1** and **2**), 1567, 1386 (**3**), 1590, 1360 (**4** · 2 CH_3OH) and 1578, 1380 cm^{-1} (**5** · CH_3OH), with the antisymmetric mode overlapping with $\nu(C{=}O)_{peptide}$ in **3** and **4** · 2 CH_3OH; this latter mode is located at 1626, 1628, 1640 for **1**, **2** and **5** · CH_3OH, respectively. The relatively large Δ value [$\Delta = \nu_{as}(COO) - \nu_s(COO)$][51] is indicative of a monodentate carboxylate coordination. The V=O stretching frequency is at 946 (**1** and **2**), 937 (**3**), 962 (**4** · 2 CH_3OH), 950 (**5** · CH_3OH) and 974 (**7**). Complex **7** has two bands at 352 and 328 cm^{-1} which are assigned to ν(V–Cl).

Magnetism and electron paramagnetic resonance spectra: The magnetic moments of compounds **1–5** · CH_3OH and **7** are 1.64, 1.61, 1.60, 1.65, 1.62 and 1.75 μ_B, respectively, at 298 K in accord with the spin-only value expected for d^1, $S = 1/2$ systems. The EPR parameters of the distorted square pyramidal (compounds **1** and **2**), the octahedral with a weak sixth ligand (compounds **3–5** · CH_3OH and **7**), and the square pyramidal compound **6** (Table 5) were determined by computer simulation of the experimental EPR spectra.

The correlation between A_z and g_z has been used to identify the coordination environment of the oxovanadium(IV) in a number of metalloproteins.[52, 53] Figure 3B is a correlation plot of A_z versus g_z, in which the A_z, g_z values were included for known oxovanadium(IV) compounds with equatorial donor atom sets O_4,[54] N_2O_2,[54] N_3O,[33] N_4,[55] N_2S_2,[56] and

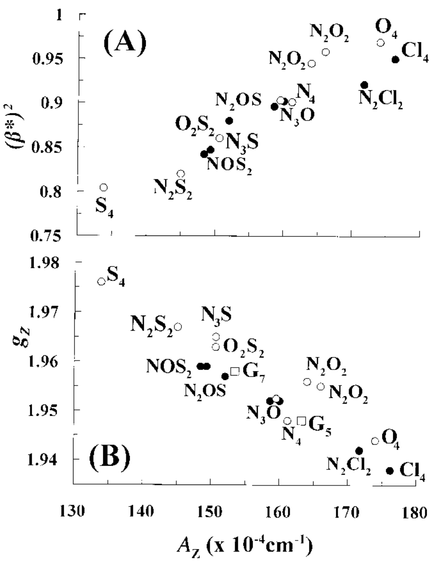

Figure 3. Correlation plots of: A) $(\beta^*)^2$ versus A_z; B) g_z versus A_z for the $V^{IV}O^{2+}$ compounds **1–7** (●) and a series of oxovanadium(IV) compounds (○) with various equatorial donor atoms. $(\beta^*)^2$ represents the population of the ground state orbital, while g_z and A_z are the principal values of the g and A tensors respectively. G_5 and G_7 (□) refer to data[27] for the $V^{IV}O^{2+}$–glutathione species at pH 5–7 and 7–10, respectively.

Table 5. Spin hamiltonian parameters for oxovanadium(IV) compounds with various coordination environments.

Compound	g_x	g_y	g_z	A_x[a]	A_y[a]	A_z[a]	g_{iso}	A_{iso}[a]	Solvent	$(\beta^*)^2$	Donor set
1	1.987	1.984	1.959	51.00	52.00	149.30	1.977	84.10	CH_2Cl_2	0.847	NOS_2
2	1.982	1.981	1.959	50.36	52.35	148.40	1.974	83.70	C_2H_5OH	0.842	NOS_2
3	1.980	1.980	1.957	48.10	53.10	152.00	1.972	84.40	C_2H_5OH	0.880	N_2OS
	1.986	1.981	1.957	50.00	52.00	150.50	1.975	84.17	CH_2Cl_2	0.862	N_2OS
4·2 CH_3OH	1.980	1.984	1.952	53.00	58.10	160.00	1.972	90.37	C_2H_5OH	0.902	N_3O
5· CH_3OH	1.984	1.980	1.952	54.50	55.00	158.60	1.972	89.37	C_2H_5OH	0.896	N_3O
6	1.978	1.978	1.938	65.00	65.00	176.20	1.965	102.07	C_2H_5OH	0.950	Cl_4
7	1.980	1.981	1.942	63.00	65.10	171.70	1.968	99.93	C_2H_5OH	0.921	Cl_2N_2
[VO(glytyr)(phen)]	1.982	1.984	1.952	53.00	58.00	160.00	1.973	90.33	C_2H_5OH	0.906	N_3O
$[VO(edt)]^{2-}$	1.978	1.977	1.976	39.7	39.7	133.8	1.977	71.1	dmf	0.834	S_4
[VO(tsalphen)]	1.987	1.987	1.967	51	51	145	1.980	82.33	dmf	0.820	N_2S_2
[VO(thipca)]	1.980	1.980	1.965	52.3	52.3	150.6	1.975	85.07	CH_2Cl_2	0.860	N_3S
$[VO(Hmpp)_2]$	1.996	1.996	1.963	51.4	51.4	150.6	1.981	80.9	dmf	0.860	O_2S_2
$[VO(bpy)_2]^{2+}$	1.981	1.981	1.948	56.42	56.42	161.19	1.970	91.34		0.901	N_4
[VO(salen)]	1.986	1.989	1.955	56.00	55.00	166.00	1.977	92.33	[b]	0.958	N_2O_2
[VO(acacen)]	1.987	1.987	1.956	55	55	164	1.977	91	[b]	0.945	N_2O_2
$[VO(acac)_2]$	1.983	1.987	1.944	62	60	174	1.971	99	$CHCl_3$	0.969	O_4

[a] Units of hyperfine coupling constants, $\times 10^{-4}$ cm^{-1}. [b] The solvent used was toluene/dichloromethane 3:7.

S_4.[57] In addition, the g_z and A_z values for **1**, **2** (NOS_2 donor set), for **3** (N_2OS donor set), for **6** (Cl_4 donor set), for **7** (N_2Cl_2 donor set), for **4**·2 CH_3OH and **5**· CH_3OH (N_3O donor set), and for [VO(thipca)] (N_3S donor set)[32] and $[VO(Hmpp)_2]$ (O_2S_2 donor set)[58] were included in Figure 3B. The equatorial donor atom sets for compounds **1**, **2**, **4**·2 CH_3OH, and **5**· CH_3OH were determined taking into account the data analyzed as described later.

The calculated ground-state orbital population parameters $(\beta^*)^2$ [52] for various oxovanadium(IV) compounds are listed in Table 5. These $(\beta^*)^2$ values were calculated by substituting the g and A values from Table 5 into Equation (8) (vide infra). The physical meaning of the parameter $(\beta^*)^2$ is such that a value of 1 would signify that the unpaired electron is localized exclusively on the vanadium d orbital, that is, that there is zero delocalization onto the ligand orbitals. On the other hand, values $(\beta^*)^2 < 1$ indicate that a fraction equal to $1-(\beta^*)^2$ of the spin density is delocalized onto the ligands. Figure 3A, which is a plot of $(\beta^*)^2$ versus A_z, allows a fundamental analysis of the experimental data. From Table 5, it is evident that the calculated $(\beta^*)^2$ values show a restricted variation between 0.82 to 0.97. This indicates that in the oxovanadium(IV) compounds listed in Table 5, the ground-state d orbitals are essentially nonbonding, in agreement with earlier reports for other oxovanadium(IV) compounds.[52, 59–61] The plot of A_z versus $(\beta^*)^2$ in Figure 3A allows us to visualize a trend, in spite of the scattering of the points. The lower $(\beta^*)^2$ values correlate with decreased A_z values. This may be better understood taking into account the general π-bonding order of the ligand donor atoms, that is, $S > N > Cl \geq O$.[52, 61] Thus, complexes with S donor atoms (sulfur atoms form π bonds quite easily) have the lowest $(\beta^*)^2$ values, compared to a compound where the vanadium atom is coordinated to chlorines. The A_z versus g_z trend (see Figure 3B) can now be explained within this model. Increased in-plane π bonding will lower the electron density at the nucleus, resulting in a decreased A_z value.[59, 61] In the same context, a delocalization through in-plane bonding will shift the g_z towards g_e, that is, it will increase g_z and at the same time lower A_z,[59, 61] and this is the reasoning for the observed anticorrelation between A_z and g_z (Figure 3B). Finally, an increased ligand covalent bonding might induce an expansion of the ground state d orbital and the inner s orbitals, and this in turn lowers the electron density at the nucleus, thus decreasing the hyperfine coupling constant.[62] In conclusion, this analysis provides a rational basis on which a plot, for example Figure 3A, may be used as a diagnostic chart for the coordination environment of oxovanadium(IV) compounds.

Table 6 lists the charge-donor atom set in the equatorial plane, the coordination number, and the $V-N_{amide}$ bond length (where it is available) for the compounds **1**–**5**· CH_3OH studied here, as well as for various oxovanadium(IV) species with amidate ligands. The $A_{z,amide}$ values were derived from the so-called additivity relationship, Equation (5), where i

$$A_{z,calcd} = \Sigma n_i A_{zi}/4 \quad (5)$$

denotes the different types of ligation to $V^{IV}O^{2+}$ equatorial donor atoms, n_i ($=1-4$) is the number of donor atoms of type i, and $A_{z,i}$ is the measured coupling constant (from model studies) when all four equatorial donor atoms are of type i. This empirical relationship is based on the experimental observation that for a given $V^{IV}O^{2+}$ compound the A_z value can be derived from the additive contributions of the A_z values of the equatorial ligands.[52] The average value for $A_{z,amide}$ is 35×10^{-4} cm^{-1} (Table 6), which is very close to the value of 34×10^{-4} cm^{-1} reported in the literature.[63] At this point, it is worth mentioning that the value of 34×10^{-4} cm^{-1} was derived from the EPR parameters of only five oxovanadium(IV) compounds (four neutral and one dianionic compound, with coordination number five, of which only three have been structurally characterized) with aromatic amides. In contrast, the value of 35×10^{-4} cm^{-1} was derived from fifteen oxovanadium(IV) compounds (nine neutral and six anionic compounds with coordination number either five or six) with either aliphatic (seven entries in Table 6) or aromatic (eight entries in Table 6) amides, of which eight have been crystallographically characterized.

The mean $A_{z,amide}$ value (Table 6) is the lowest reported value among various nitrogen donor atoms [e.g., $A_{z,R-NH_2}=$

Table 6. Correlation between $A_{z,amide}$, charge-donor atom set in the equatorial plane, coordination number and V-N_{amide} bond lengths for various oxovanadium(IV) compounds with amidate ligands.

Compound	Charge, donor atom set of the complexed ligand	Coordination number	V–N_{amide} [Å]	$A_{z,amide}$ [10^{-4} cm^{-1}][c]	Ref.
[VO(bpb)]	–2, N_4	5[a]		32	[63]
[VO(phepca)]	–2, N_3O	5[a]	1.989(4)	30	[63]
[VO(pycac)]	–2, N_3O	5[a]	1.979(5)	29	[64]
[VO(pycbac)]	–2, N_3O	5[a]	1.989(2)	30	[64]
[VO(thipca)]	–2, N_3S	5[a]	1.997(3)	31	[32]
4 · 2 CH_3OH	–2, N_3O	6[b]		35	this work
5 · CH_3OH	–2, N_3O	6[b]		34	this work
[VO(glyphe)(phen)]	–2, N_3O	6[b]		34	[33]
[VO(glytyr)(phen)]	–2, N_3O	6[b]	1.927(7)	35	[33]
$[VO(hypyb)]^-$	–3, N_3O	5[a]	2.009(8)	38	[32]
3	–3, N_2OS	6[b]	1.997(4)	35[d]	this work
$[VO(hymeb)]^{2-}$	–4, N_2O_2	5[b]		37	[63]
$[VO(hybeb)]^{2-}$	–4, N_2O_2	5[a]	2.022(15)	39	[32]
1	–4, NOS_2	5[a]		43	this work
2	–4, NOS_2	5[a]		42	this work
Mean				35	

[a] Aromatic amides. [b] Aliphatic amides. [c] The $A_{z,i}$ values for $i = R{-}CO_2^-$, =N- (aromatic imine), $R{-}NH_2$, $Ar{-}O^-$, $R{-}O^-$, $Ar{-}S^-$, $R{-}S^-$ were derived from oxovanadium(IV) compounds reported in ref. [52] and are 42.7, 40.7, 40.1, 38.9, 35.3, 35.3, and 31.9×10^{-4} cm^{-1} respectively. The $A_{z,i}$ values for $i = Cl^-$, =N- [aromatic imine, i.e., the phenanthroline nitrogen], =N- [aliphatic imine] and =C–O^- (acac-type O^-) were derived from compounds **6** (ref. [68]), **7**(ref. [69]), [VO(salen)] (ref. [54]), and [VO(acacen)] (ref. [54]) and are 44.1, 41.80, 44.1, and 37.9×10^{-4} cm^{-1} respectively. All the above $A_{z,i}$ values were used to calculate the contribution of a deprotonated amide nitrogen to A_z, i.e., the $A_{z,amide}$ for the oxovanadium(IV) compounds. [d] This is the average $A_{z,amide}$ value in the two solvents used.

40.1×10^{-4} cm^{-1}, $A_{z,N-(aliphatic\ imine)} = 44.4 \times 10^{-4}$ cm^{-1}, $A_{z,N-(aromatic\ imine)} = 40.7 \times 10^{-4}$ cm^{-1}, etc.],[52] but it is equal to $A_{z,R-O^-}$ and $A_{z,R-S^-}$ which are both $\approx 35 \times 10^{-4}$ cm^{-1}, and it approaches the value for a thiolate sulfur A_{z,RS^-}, $\approx 32 \times 10^{-4}$ cm^{-1}. This last A_z value is the lowest $A_{z,i}$ value reported in the literature. Low $A_{z,i}$ values reflect a reduced electron–nuclear hyperfine interaction, which results from a reduced unpaired spin density at the ^{51}V nucleus (vide supra). Amongst other factors, increased in-plane π bonding or delocalisation through in-plane σ bonding will decrease the A_z value. *N*-coordinated organic amidate ligands are known to be strong donors to transition metal centers.[65–67] Thus, it is evident that the observed low $A_{z,amide}$ values reflect a strong covalent bonding between the deprotonated amide nitrogen and the oxovanadium(IV) center. Such strong covalency requires the availability of ligand orbitals that can π-bond with the empty d orbitals (vide supra) of the vanadium. Electron spin echo envelope modulation (ESEEM)[70–73] experiments that are currently being performed corroborate this view; these will be published in the near future.

A comparison of the V–N_{amide} bond lengths with the corresponding $A_{z,amide}$ values (Table 6) does not reveal any apparent correlation, though one might expect that as the V–N_{amide} bond becomes stronger, the $A_{z,amide}$ value should be reduced. Accumulation of more data might clarify the situation.

It is evident from Table 6 that the $A_{z,amide}$ value is not a fixed quantity for an isolated deprotonated amide nitrogen (it varies from 29 to 43×10^{-4} cm^{-1}), but is affected by the presence of the three other donor atoms in the equatorial plane and in particular by their charge. Thus, when the charge of the donor atoms in the equatorial plane is –2 (including the –1 charge of the deprotonated amide nitrogen) and the coordination number of the vanadium(IV) species is five, the $A_{z,amide}$ value is $\approx 30 \times 10^{-4}$ cm^{-1}, while coordination number six results in an average $A_{z,amide}$ value of $\approx 35 \times 10^{-4}$ cm^{-1}. When the charge of the donor atoms in the equatorial plane is –3 the $A_{z,amide}$ value is $\approx 37 \times 10^{-4}$ cm^{-1} and finally when it is –4 the $A_{z,amide}$ is $\approx 40 \times 10^{-4}$ cm^{-1}. Although there are not enough data for the last two cases (–3 and –4), it appears that the $A_{z,amide}$ value is sensitive to the charge of equatorial donor atoms. So, one has to be very cautious in using the average $A_{z,amide}$ value unless the charge of the equatorial donor atoms is known.

Addition of the EPR parameters[27] (g_z-A_z), for the system $V^{IV}O^{2+}$–glutathione at pH 5–7 ($g_z = 1.948$, $A_z = 163 \times 10^{-4}$ cm^{-1}) and pH 7–10 ($g_z = 1.959$, $A_z = 154 \times 10^{-4}$ cm^{-1}) on the correlation plot A_z versus g_z (Figure 3B) shows that the most reasonable equatorial coordination environment for the oxovanadium(IV) species might be an N_2O_2 (the A_z value for the N_2O_2 system [VO(acacen)] (Table 5) is 164×10^{-4} cm^{-1}) and an N_2OS (the A_z value for the N_2OS system **3** (Table 5) is 152×10^{-4} cm^{-1}) for pH 5–7 and 7–10, respectively. On the basis of the additivity relationship, the calculated A_z value for the vanadium–glutathione species with an N_2O_2 donor atom set is 165.6×10^{-4} cm^{-1} with proposed equatorial coordination [2 RNH_2, 2 $RCOO^-$], which is very close to the experimental value of 163×10^{-4} cm^{-1}, while the calculated A_z value for the N_2OS donor set is 154.6×10^{-4} cm^{-1} with proposed equatorial coordination [1 $RCOO^-$, 2 -CON^--, 1 R–S^-], which is almost identical to the experimental value of 154×10^{-4} cm^{-1}. On the basis of the above discussion the possible structures of $V^{IV}O^{2+}$–glutathione compounds at various pHs are depicted in Figure 4.

Proposed structures for compounds 1, 2, 4 · 2 CH_3OH, and 5 · CH_3OH: The $(\beta^*)^2$, g_z, and A_z values, as well as the electrochemical properties (CV and polarography) and UV–VIS spectra, for compounds **4** · 2 CH_3OH and **5** · CH_3OH are almost identical (Table 5 and Figure 3) to those reported for the very similar compound [V^{IV}O(glytyr)(phen)][33] (**8**). Since compound **8** has been crystallographically characterized, it is reasonable to assume that the equatorial donor atom set in both compounds is N_3O. On the other hand, application of the additivity relationship for compounds **4** · 2 CH_3OH and **5** · CH_3OH gives a calculated A_z value of 160×10^{-4} cm^{-1} with proposed equatorial coordination [1 RNH_2, 1 CON^-, 1 $RCOO^-$, 1 N_{phen}], which is identical to the experimental A_z value of 160×10^{-4} cm^{-1} for **4** · 2 CH_3OH and very close to the value of 158.6×10^{-4} cm^{-1} for **5** · CH_3OH. The N_3O

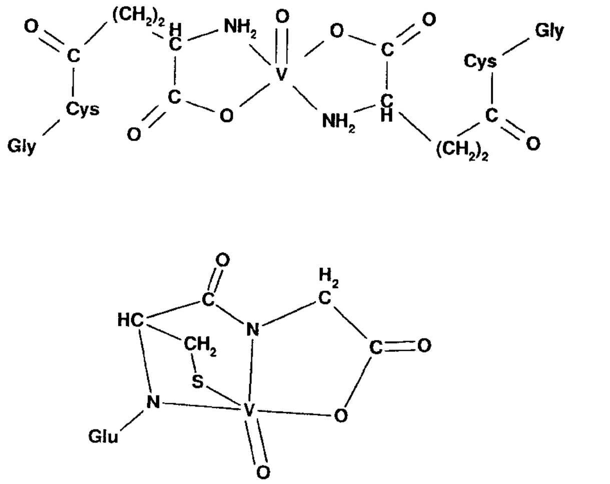

Figure 4. Possible structures for $V^{IV}O^{2+}$ with glutathione at pH = 5 – 7 (top) and pH = 7 – 10 (bottom).

equatorial donor atom set was confirmed from ESEEM experiments, which indicate that the $V^{IV}O^{2+}$ center binds to an amine,[74] an amide,[74] and one phenanthroline nitrogen[74] atom.

Addition of the $(\beta^*)^2$, g_z, and A_z values for compounds **1** and **2** on the correlation plots A_z versus $(\beta^*)^2$ (Figure 3A) and A_z versus g_z (Figure 3B) reveals that these compounds have an intermediate ligand-field strength between (N_3S and O_2S_2) and N_2S_2 donor types. The additivity relationship for A_z gives a calculated A_z value of $\approx 147 \times 10^{-4}\,cm^{-1}$, with proposed equatorial coordination [1 $RCOO^-$, 1 -CON^--, 2 R – S^-], that is, quite close to the experimental A_z values for both compounds (149.30 and $148.40 \times 10^{-4}\,cm^{-1}$ for **1** and **2**, respectively). ESEEM experiments reveal that a deprotonated amide nitrogen[74] coordinates to the $V^{IV}O^{2+}$ center for **1** and **2**. Thus, the most reasonable equatorial donor atom set is NOS_2 for **1** and **2**. The proposed structures for **1** and **4** on the basis of the above data are shown in Figure 5. The structures of **2** and **5** resemble those of **1** and **4**, respectively.

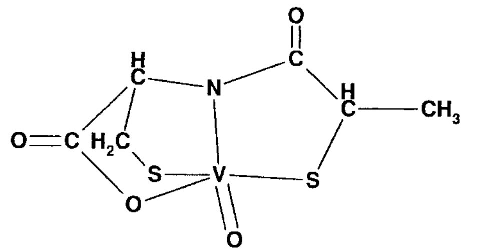

[$V^{IV}O(m_2pc)]^{2-}$ (Anion of 1)

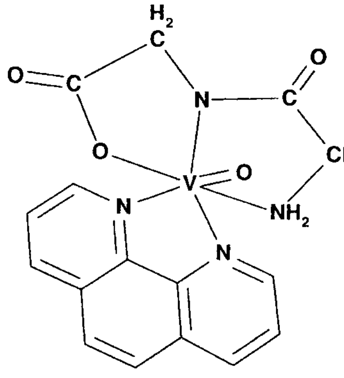

[$V^{IV}O$(glygly)(phen)] (4)

Figure 5. Proposed structures for $[V^{IV}O(m_2pc)]^{2-}$ (anion of **1**) and [$V^{IV}O$(glygly)(phen)] (**4**).

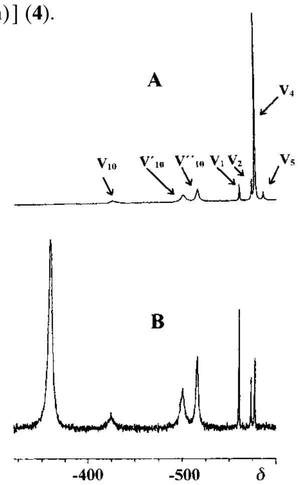

Figure 6. ^{51}V NMR spectra showing: A) the spectrum of $NaVO_3$ and B) the result after the addition of H_3mpg. The signal at $\delta = -359$ is due to the complex formation. Conditions: A) 40 mM vanadate, pH 6.5, 278 K; B) 20 mM vanadate, 20 mM H_3mpg, pH 6.5, 278 K; $\approx$25 mM NaCl.

NMR spectroscopy: The ^{51}V NMR spectrum of an aqueous solution containing 20 % D_2O, 20 mM $NaVO_3$, and 20 mM H_3mpg at pH = 6.5 shows the formation of 60 % of a new vanadium(v) complex ($\delta = -359$) (Figure 6). The hydrolytic stability of the complex was studied over the pH range 3.5 – 6.5, and it was found that the highest [complex]/[vanadate monomer] ratio was obtained at pH = 6.5. The chemical shift of $\delta = -359$ in the ^{51}V NMR spectrum reveals that at least one soft donor atom (sulfur) is coordinated to vanadium.[75] The ^1H NMR spectrum of the same solution was also recorded and showed the formation of $\approx$65 % of the complex (Figure 7). This means that the [vanadium]/[ligand] ratio is 1:1 in the complex. ^1H and ^{13}C NMR spectroscopy was used to determine the type of coordinated moieties in the vanadium(v) complex. Both spectroscopic methods are very sensitive to complexation, because a simple change in the electronic environment of either a ^1H or a ^{13}C nucleus affects the chemical shift. The full assignment of the proton and carbon atoms of the free ligand and its vanadium(v) complex, as well as the coordination-induced shift (CIS) values, are reported in Table 7. The CIS value for a given nucleus is defined as the difference between its chemical shift in the complex versus that in the free ligand, CIS = $\delta_{bound} - \delta_{free}$. Four carbon resonances in the vanadium(v) complex show significant shifts from the free ligand: the carboxylate carbon (+ 7.66 ppm), the carbonyl carbon in the amide group (+ 11.21 ppm), the -CH_2- group in the glycine moiety (+ 11.84 ppm) and the -CH- group in the 2-mercaptopropionic acid moiety (+ 7.07 ppm). In addition, the carbon atom in the CH_3- group (Scheme 1) shows a significant shift (+ 1.85 ppm). On the basis of these data, we conclude that the vanadium(v) atom is ligated to a tridentate ligand at the $S_{thiolato}$ atom, the $N_{peptide}$ atom, and one of the $O_{carboxylato}$ atoms.[76–78]

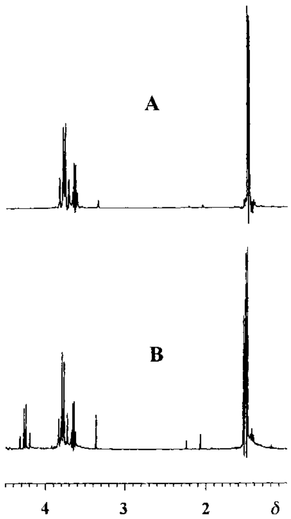

Figure 7. ^1H NMR spectra of H_3mpg. A) prior to and B) after the addition of $NaVO_3$. Conditions: A) 40 mM H_3mpg, pH 6.5, 278 K; B) 20 mM H_3mpg, 20 mM vanadate, pH 6.5, 278 K; ≈25 mM NaCl.

Table 7. ^1H and ^{13}C NMR chemical shifts of the ligand H_3mpg, its vanadium(V) compound, and the CIS values.

	H_3mpg		V^V–mpg^{3-}		CIS	
	^1H	^{13}C	^1H	^{13}C	^1H	^{13}C
$-CH_2-$	3.78	46.34	4.25	58.18	+0.47	+11.84
$-CH-$	3.62	39.71	3.83	46.78	+0.21	+7.07
$-CH_3$	1.48	23.56	1.52	25.41	+0.04	+1.85
$-COOH$	–	179.50	–	187.16	–	+7.66
$-CO-$	–	179.54	–	190.75	–	+11.21
$-NH-$	8.36	–	[a]	–	–	–

[a] Not observed.

A combination of ^{51}V and ^1H NMR spectroscopy was used to monitor the reduction of the vanadium(V) species to vanadium(IV). This combination showed that there was no reduction of V(V) to V(IV) two hours after the preparation of the sample and only 20% of the total vanadium(V) was reduced to vanadium(IV) 24 h later.

Since a part of glutathione is similar to H_3mpg (Scheme 1), it is reasonable to assume that glutathione could interact with vanadate in a similar way.

Conclusions

Oxovanadium(IV)–glutathione model compounds were synthesized and characterized by a variety of techniques in order to obtain structural information relating to the $V^{IV}O^{2+}$–glutathione system. This study reveals that the $V^{IV}O^{2+}$ center might form various species with glutathione inside the cells, but these species, at physiological pH, are unstable, since at pH ≥ 6.5 there is a potential for deprotonation of the peptide nitrogens and thiol sulfur of glutathione, comparable to the situation for the model compounds reported here. Model NMR studies (interaction of vanadium(V) with H_3mpg; ^1H, ^{13}C and ^{51}V) showed that there is a possibility of vanadium(V) ligation to glutathione at physiological pH, which is then followed by reduction of vanadium(V) to vanadium(IV).

The plot of A_z versus $(\beta^*)^2$ provides a correlation between the bonding properties (expressed by the value of $(\beta^*)^2$) of the equatorial donor atoms and the experimental EPR parameters (A_z) of the oxovanadium(IV) compound. The plot of A_z versus g_z is an empirical correlation between these two experimental parameters and has been used as a benchmark to identify the coordination environment of the vanadium atom. The comparative analysis adopted here provides a link between these two methods of data analysis, that is, $(\beta^*)^2$ versus A_z and g_z versus A_z. Combination of the correlation plot g_z versus A_z or $(\beta^*)^2$ versus A_z with the additivity relationship (which is valid even for highly distorted square pyramidal geometry towards trigonal bipyramidal geometry[79] and for octahedral geometry with a weak sixth ligand),[57, 68] is a powerful technique for probing the equatorial donor atoms in an oxovanadium(IV) compound and consequently, in biomolecules (e.g., vanadoproteins and oxovanadium(IV)-substituted proteins, etc.). Thus, for the $V^{IV}O^{2+}$–glutathione system, combination of the correlation plot g_z versus A_z with the additivity relationship helped us to propose the possible structures of the $V^{IV}O^{2+}$–glutathione species at various pH values.

The contribution of a deprotonated peptide (amide) nitrogen to A_z (based on the additivity relationship) is not a fixed quantity (it varies from 29 to 43×10^{-4} cm^{-1}), but it is affected by the presence of the three other donor atoms in the equatorial plane and, in particular, their charge. Thus, when the charge of the donor atoms in the equatorial plane is −2, −3, or −4 (including the −1 charge of the deprotonated peptide nitrogen) the mean $A_{z,peptide}$ value is 30×10^{-4} (square pyramidal geometry) or 35×10^{-4} (octahedral geometry), 37×10^{-4}, and 40×10^{-4} cm^{-1}, respectively.

Experimental Section

Materials and synthesis of the oxovanadium(IV) compounds: Bis(acetato)oxovanadium(IV), $[VO(CH_3COO)_2]$,[80] dichlorobis(tetrahydrofuran)oxovanadium(IV), $[VOCl_2(thf)_2]$,[81] bis(pentane-2,4-dionato)oxovanadium(IV), $[VO(acac)_2]$,[82] and tetraethylammonium perchlorate[64] were prepared by literature procedures. The purity of the above-mentioned compounds was confirmed by elemental analyses (C,H,N) and infrared spectroscopy. Reagent grade dichloromethane, acetonitrile, triethylamine, and nitromethane were dried and distilled over powdered calcium hydride, while toluene and diethyl ether were dried and distilled over sodium wire. Methanol and ethanol were dried by refluxing over magnesium methoxide and ethoxide, respectively. Syntheses, distillations, crystallization of the oxovanadium(IV) compounds, and spectroscopic characterization were performed under high-purity argon by standard Schlenk techniques. C, H, N, and S analyses were conducted by the University of Ioannina's microanalytical service, vanadium was determined gravimetrically as vanadium pentoxide or by atomic absorption, and chloride analyses were carried out by potentiometric titration.

Bis(triethylammonium) [*N*-(2-mercaptopropionyl)cysteinato-*O,S,N,S*] oxovanadate(IV), $[(Et_3NH)]_2[VO(m_2pc)]$ (1): To a stirred suspension of $[VO(CH_3COO)_2]$ (0.200 g, 1.08 mmol) in acetonitrile (15 mL) was added in one portion solid 1,10-phenanthroline (0.195 g, 1.08 mmol). The mixture was refluxed for ≈3 h, after which the pale green color of the solid changed to yellow. Then the solution was cooled to room temperature and H_4m_2pc (0.226 g, 1.08 mmol) and triethylamine (0.547 g, 5.40 mmol) were added to the mixture. After being stirred for 24 h, the precipitate was dissolved and the pale green color of the solution turned to deep purple. Filtration and evaporation of the solution to dryness under vacuum gave a gum. Diethyl ether (20 mL) was added and the mixture was magnetically stirred for ≈4 h to give a purple precipitate, which was filtered off and triturated with toluene (2 × 30 mL), and filtered again, washed with diethyl ether (2 × 5 mL) and dried in vacuo to yield 0.23 g of **1** (45%). Elemental analysis:

$C_{18}H_{39}N_3O_4S_2V$ (476.58), calcd C 45.36, H 8.25, N 8.82, S 13.46, V 10.69; found C 45.32, H 8.26, N 8.84, S 13.42, V 10.68.

Bis(triethylammonium) [*N*-(3-mercaptopropionyl)cysteinato-*O,S,N,S*] oxovanadate(IV), [$(Et_3NH)]_2$[VO($m_3$pc)] (2): Compound **2** was prepared in 42% yield by a similar procedure to that of **1** but with H_4m_3pc in place of H_4m_2pc. Elemental analysis: $C_{18}H_{39}N_3O_4S_2V$ (476.58), calcd C 45.36, H 8.25, N 8.82, S 13.46, V 10.69; found C 45.38, H 8.24, N 8.80, S 13.44, V 10.71.

Triethylammonium [*N*-(2-mercaptopropionyl)glycinato-*O,N,S*](1,10-phenanthroline) oxovanadate(IV), [Et_3NH][VO(mpg)(phen)] (3):

Method A: 1,10-Phenanthroline (0.192 g, 1.06 mmol) was added to a stirred solution of [$VOCl_2(thf)_2$] (0.300 g, 1.06 mmol) in acetonitrile (≈7 mL) at room temperature (≈30°C). An immediate color change from blue to green concurrent with the precipitation of a green solid was observed. Sequential addition of H_3mpg (0.174 g, 1.06 mmol) and triethylamine (0.538 g, 5.32 mmol) to the mixture induced a sequence of color changes (from green through brown to purple) accompanied by dissolution of the green precipitate and the formation of a purple solid. The mixture was stirred for ≈2 h, filtered, and the purple compound washed with cold acetonitrile (2 × 5 mL) and diethyl ether (2 × 15 mL) and dried in vacuo to afford 0.43 g of **3** (80%). Elemental analysis: $C_{23}H_{30}N_4O_4SV$ (509.52), calcd C 54.22, H 5.93, N 11.00, S 6.29, V 10.00; found C 54.15, H 5.90, N 10.85, S 6.15, V 10.01.

Method B: Solid 1,10-phenanthroline (0.340 g, 1.89 mmol) was added in one portion to a stirred suspension of [$VO(acac)_2$] (0.500 g, 1.89 mmol) in acetonitrile (≈15 mL). The solution cleared and its color changed from blue to olive green. H_3mpg (0.308 g, 1.89 mmol) was added to the stirred solution, whereupon a yellow precipitate was formed and the solution became deep yellow-brown. Then triethylamine (0.935 g, 9.24 mmol) was added to the mixture, which was stirred overnight, and a purple precipitate was formed and the color of the solution became red-brown. The solid was filtered off, washed with dichloromethane (≈5 mL) and diethyl ether (2 × 15 mL), and dried in vacuo to yield 0.30 g (32%) of product.

(Glycylglycinato-*O,N,N*)(1,10-phenanthroline)oxovanadium(IV), [VO(glygly)(phen)]·2CH$_3$OH (4·2CH$_3$OH): Compound **4**·2CH$_3$OH was prepared in a fashion similar to that for complex **3** except that i) methanol was used as solvent; ii) the reaction time was ≈3 h, and iii) H_2glygly was used instead of H_3mpg. The product was obtained in 63% yield. Elemental analysis for **4**·2CH$_3$OH: $C_{18}H_{22}N_4O_6V$ (441.33) calcd C 48.99, H 5.02, N 12.70, V 11.54; found C 48.70, H, 4.89, N 12.85, V 11.44.

(Glycyl-L-alanilato-*O,N,N*)(1,10-phenanthroline)oxovanadium(IV), [VO(glyala)(phen)]·CH$_3$OH (5·CH$_3$OH): Compound **5**·CH$_3$OH was synthesized in an analogous fashion to complex **4**·2CH$_3$OH, except that H_2glyala was used instead of H_2glygly in 70% yield. Elemental analysis for **5**·CH$_3$OH: $C_{18}H_{20}N_4O_5V$ (423.32) calcd C 51.07, H 4.76, N 13.25, V 12.03; found C 51.01, H 4.75, N 13.20, V 12.24.

Bis(tetraethylammonium) tetrachlorooxovanadate(IV), [$(Et_4N)_2$][$VOCl_4$] (6): Solid Et_4NCl (0.470 g, 2.84 mmol) was added to a stirred suspension of [$VOCl_2(thf)_2$] (0.400 g, 1.42 mmol) in dichloromethane (30 mL) in one portion at room temperature. After the mixture had been stirred overnight, the light blue solution had changed to almost colorless, and the light blue precipitate had redissolved and a blue-green solid formed. This product was filtered off and washed with diethyl ether (2 × 5 mL) and dried in vacuo to afford 0.56 g of **6** (84%). Elemental analysis for **6**: $C_{16}H_{40}N_2OCl_4V$ (469.25) calcd C 40.95, H 8.59, Cl 30.22, N 5.97, V 10.86; found C 40.92, H 8.61, Cl 30.30, N 5.99, V 10.85.

***cis*-Dichloro(methanol)(1,10-phenanthroline)oxovanadium(IV), [$VOCl_2$(CH$_3$OH)(phen)] (7)**: Solid 1,10-phenanthroline (0.192 g, 1.06 mmol) was added in one portion to a stirred solution of [$VOCl_2(thf)_2$] (0.300 g, 1.06 mmol) in methanol. Immediately upon addition of 1,10-phenanthroline the blue solution became green. Then over 2 h of magnetic stirring a green precipitate was formed, which was filtered off (crystals of **7** suitable for X-ray structure analysis were obtained by vapor diffusion of diethyl ether into the filtrate), washed with diethyl ether (2 × 5 mL), and dried in vacuo to afford 0.26 g of green product (70%). Elemental analysis for **7**: $C_{13}H_{12}N_2O_2Cl_2V$ (350.09), calcd C 44.60, H 3.46, Cl 20.25, N 8.00, V 14.55; found C 44.62, H 3.47, Cl 20.18, N 8.01, V 14.57.

X-ray crystallography:

*Complex **3**·MeOH*: A crystal with approximate dimensions 0.10 × 0.25 × 0.35 mm was mounted in air and covered with epoxy glue. Diffraction measurements were made on a $P2_1$ Nicolet diffractometer upgraded by Crystal Logic, with Ni-filtered Cu radiation. Unit cell dimensions were determined and refined by using the angular settings of 25 automatically centered reflections in the range $22 < 2\theta < 52$; they appear in Table 8. Intensity data were recorded with a $\theta-2\theta$ scan to $2\theta_{max} = 115°$ with scan speed 1.5° min^{-1} and scan range 2.5 plus $\alpha_1\alpha_2$ separation. Three standard reflections monitored every 97 reflections showed less than 3% variation and no decay. Lorentz, polarization, and ψ-scan absorption corrections were applied with Crystal Logic software. Symmetry-equivalent data were averaged with $R = 0.0219$ to give 3579 independent reflections from a total of 3767 collected. The structure was solved by direct methods by SHELXS-86 and refined by full-matrix least-squares techniques on F^2 with SHELXL-93 using 3577 reflections and refining 352 parameters. The crystal was of poor quality. Hydrogen atoms of the phenanthroline were located by difference maps, the rest were introduced at calculated positions as riding on bonded atoms. All nonhydrogen atoms (except those of the solvent methanol, which were refined isotropically with occupation factor fixed at 10.5) were refined anisotropically.

The final values for R, R_w and GoF for observed data are given in Table 8, and for all data values are 0.0757, 0.1778, and 1.048, respectively. The maximum and minimum residual peaks in the final difference map were 0.373 and −0.308 Å^3. The largest shift/esd in the final cycle was 0.003.

*Complex **7***: A crystal with approximate dimensions 0.10 × 0.25 × 0.70 mm was mounted in air and covered with epoxy glue. Diffraction measurements were made on a Crystal Logic dual goniometer diffractometer with graphite-monochromated Mo radiation. Unit cell dimensions were determined and refined by using the angular settings of 25 automatically centered reflections in the range $11 < 2\theta < 23$, and they appear in Table 8. Intensity data were recorded using a $\theta-2\theta$ scan to $2\theta_{max} = 47°$ with scan speed 2.5 deg min^{-1} and scan range 2.3 plus $\alpha_1\alpha_2$ separation. Three standard reflections monitored every 97 reflections showed less than 3% variation and no decay. Lorentz, polarization, and ψ-scan absorption correction were applied by means of Crystal Logic software. Symmetry-equivalent data were averaged with $R = 0.0108$ to give 2161 independent reflections from a of total 2239 collected. The structure was solved by direct methods with SHELXS-86 and refined by full-matrix least-squares techniques on F^2 with SHELXL-93 using 2161 reflections and refining 229 parameters. All hydrogen atoms were introduced at calculated positions as riding on bonded atoms. All nonhydrogen atoms were refined anisotropically. The final values for $R1$, $wR2$, and GoF for observed data are in Table 8; values for all the data are 0.0580, 0.1193, and 1.150, respectively. The maximum and minimum residual peaks in the final difference map were 0.351 and −0.374 e Å^{-3}. The largest shift/esd in the final cycle was 0.005. Final atomic coordinates are listed in the Supporting Information in Tables S1,S2 for nonhydrogen atoms and in Tables S3,S4 for hydrogen atoms. Thermal parameters are given in Tables S5,S6, bond lengths and angles in Tables S7,S8. Crystallographic data (excluding structure factors) for the structures reported in this paper have been deposited with the Cambridge Crystallographic Data Center as supplementary publication no. CCDC-112747 and 112748 for **3**·CH$_3$OH and **7**, respectively. Copies of the data can be obtained free of charge on application to CCDC, 12 Union Road, Cambridge CB2 1EZ, UK (fax: (+44) 1223-336-033; e-mail: deposit@ccdc.cam.ac.uk).

Physical measurements: Infrared spectra of the various compounds dispersed in KBr pellets were recorded on a Perkin–Elmer 577 spectrometer. A polystyrene film was used to calibrate the frequency. Electronic absorption spectra were measured as solutions in septum-sealed quartz cuvettes at ≈ −15°C on a Jasco V-570 UV/Vis–NIR spectrophotometer. Magnetic moments were measured at room temperature by the Faraday method, with mercuric tetrathiocyanatocobaltate(II) as the susceptibility standard on a Cahn–Ventron RM-2 balance.

EPR studies: Continuous-wave EPR[83] spectra were recorded at liquid helium temperatures with a Bruker ER 200D X-band spectrometer equipped with an Oxford Instruments cryostat. The microwave frequency and the magnetic field were measured with a microwave-frequency counter HP 5350B and a Bruker ER 035M NMR gaussmeter, respectively. The temperature was monitored with an Oxford ITC5 temperature controller equipped with a calibrated AuFe (0.007 Chr) thermocouple. For the EPR measurements the oxovanadium(IV) compounds were dissolved in ethanol or dichloromethane at ≈ −15°C with subsequent freezing in liquid nitrogen. The program SIMFONIA version 2.1 by Bruker was used for numerical simulation of the EPR spectra, for an $S = 1/2$ electron spin coupled to the $I = 7/2$ nuclear spin from the ^{51}V nucleus. No resolvable improvement of the simulations could be achieved by considering noncollinear g and hyperfine tensor A; thus these two tensors are considered to be collinear.

Calculation of the ground-state orbital population from EPR data: The fundamental parameters that are calculated from the EPR spectra are the three principal values of the g tensor (g_x,g_y,g_z) and the ^{51}V hyperfine coupling tensor A (A_x,A_y,A_z). Typically, the oxovanadium(IV) compounds possess a strong axial symmetry around the V=O bond, thus leading to axial $g = (g_\perp, g_\perp, g_\parallel)$ and A ($A_\perp, A_\perp, A_\parallel$) values. For axially symmetric EPR spectra, the expressions relating the hyperfine coupling constants to the molecular orbital parameters and the electronic transitions are given in Equations (6) and (7).[52]

$$A_\parallel = PK - 4/7(\beta^*)^2P - (g_e - g_\parallel)p - 3/7(g_e - g_\perp)P \quad (6)$$

$$A_\perp = -PK + 2/7(\beta^*)^2P - 11/14(g_e - g_\parallel)P \quad (7)$$

In these equations g_e equals 2.0023, and is the free-electron g value; $P = 2.0023 g_N \beta_e \beta_N \langle r^{-3}\rangle$ is the dipole–dipole interaction between the electron and nuclear moment. In the calculation a value of $P = 0.00125\ \mathrm{cm^{-1}}$[59, 61] was used. K is the Fermi contact term, which is related to the amount of unpaired s-electron density at the vanadium nucleus. The parameter $(\beta^*)^2$ represents the population of the ground-state d orbital. For C_{4v} symmetry, $(\beta^*)^2$ is the vanadium $|d_{xy}\rangle$ orbital population[48, 84] ($|d_{x^2-y^2}\rangle$ for C_{2v} symmetry).[85] In the case of rhombic spectra, the Equations (6) and (7) are still valid, assuming that the mixing of the states is negligible, and setting $A_\perp = (A_x + A_y)/2$ and $g_\perp = (g_x + g_y)/2$, $g_\parallel = g_z$ and $A_\parallel = A_z$.[48, 84, 85] Equation (8) is derived from Equations (6) and (7).

$$(\beta^*)^2 = 4/7(A_\perp - A_\parallel)/P + (g_e - g_\parallel) - 5/14(g_e - g_\perp) \quad (8)$$

Electrochemistry: Electrochemical experiments were performed with a Metrohm E629 Polarecord-VA-Scanner E612 apparatus connected to a Houston 2000XY recorder. Platinum disk and dropping mercury electrodes (DME) were employed as working electrodes for the cyclic voltammetric and polarographic studies, respectively. A platinum wire was used as an auxiliary electrode, while a silver/silver chloride electrode in dichloromethane (saturated with tetrabutylammonium tetrafluoroborate) or acetonitrile (saturated with tetraethylammonium perchlorate) was used as a reference electrode. The supporting electrolytes in dichloromethane and acetonitrile were tetrabutylammonium tetrafluoroborate and tetraethylammonium perchlorate (0.1 M) respectively, and all solutions were 10^{-3}–10^{-4} M in vanadium compound. Values for the reduction potential ($E_{1/2}$) and the number of electrons involved in the reversible process were obtained from the intercept and the slope of the plot of $\ln[(i_d - i)/i]$ versus potential (E) according to the Heyrovsky–Ilkovic equation[86] [Eq. (9)]. All

$$E = E_{1/2} + (RT/\eta F)\{\ln[(i_d - i)/i]\} \quad (9)$$

potentials throughout this paper are relative to the normal hydrogen electrode (NHE);[87] ferrocene (+0.400 V vs. NHE)[88] was used as a standard. The cyclic voltammetric studies were recorded at $\approx -15\,^\circ$C, while the polarographic studies were recorded at $\approx 10\,^\circ$C.

NMR spectroscopy and sample preparation: NMR spectra were recorded on Bruker AMX 400 spectrometer at 278 K. Routine parameters were used when recording the ^{1}H and ^{13}C spectra. The chemical shifts are reported with respect to DDS as external standard.

The ^{51}V NMR spectra were recorded at 105 MHz, using a sweep width of about 150000 Hz, a pulse angle of 90°, and a relaxation time of 0.2 s. The ^{51}V NMR spectra are referenced to external $VOCl_3$. An exponential line broadening of 20 Hz was imposed on the accumulated data prior to Fourier transformation, at which point each ^{51}V NMR spectrum was phased, baseline-corrected and integrated.

^{13}C NMR spectra were obtained at 100.6 MHz and the assignment of the peaks was based on ^{1}H, ^{13}C HMQC, and HMBC experiments (gradient version). These spectra were acquired with 2K × 256 points, 16 and 48 scans per increment, respectively. The t_1 dimension was zero-filled to 512 real data points and 0° square cosine-bell window functions were applied in both dimensions.

Stock solutions of $NaVO_3$ (40 mM) and H_3mpg (40 mM) were prepared at room temperature by dissolving the solid materials in D_2O or in distilled and deionized H_2O containing 20% (v/v) D_2O. Three freeze–thaw cycles were used to degas the solvent. The pH of these solutions was adjusted to 6.5 with the addition of HCl (2 M) or NaOH (2 M). When HCl was used, the stock solution immediately turned yellow-orange, indicating the presence of vanadate decamer. Such solutions were stored until the yellow-orange color had almost disappeared.[89] The NMR samples were prepared at ambient temperature by mixing appropriate volumes of the $NaVO_3$ and H_3mpg stock solutions. The NMR spectra were recorded immediately after preparation of the samples, and not beyond 2 h after their preparation.

Acknowledgements

We gratefully acknowledge support of this research by the Greek General Sectetariat of Research and Technology (Grant no. 1807/95) and the General Secretariat of Athletics (OPAP); we thank A. Athanasiou and F. Masala for typing the manuscript.

[1] M. Anke, B. Groppel, K. Gruhn, T. Kosla, M. Szilagyi, in *Spurelement-Symposium: New Trace Elements* (Eds.: M. Anke, W. Bauman, H. Braunlich, C. Bruckner, B. Groppel), Friedrich-Schiller-Universität, Jena, pp. 1266–1275; E. O. Uthus, F. H. Nielsen, *FASEB J.* **1988**, 2, A841.
[2] B. F. Harland, B. A. Harden-Williams, *J. Am. Diet Assoc.* **1994**, *94*, 891.
[3] D. Rehder, in *Metal Ions in Biological Systems, Vol. 31* (Eds.: H. Sigel, A. Sigel), Marcel Dekker, New York, **1995**, pp. 1–43.
[4] B. R. Nechay, *Annu. Rev. Pharmacol.* **1984**, *24*, 501.
[5] G. Swarup, K. V. Speeg, S. Cohen, D. L. Garbers, *J. Biol. Chem.* **1982**, *257*, 7298.
[6] A. Evangelou, S. Karkabounas, G. Kalpouzos, M. Malamas, R. Liasko, D. Stefanou, A. T. Vlahos, T. A. Kabanos, *Cancer Lett.* **1997**, *119*, 221.
[7] C. Orvig, K. H. Thompson, M. Battel, J. H. McNeil, in *Metal Ions in Biological Systems*, *Vol. 31* (Eds.: H. Sigel, A. Sigel), Marcel Dekker, New York, **1995**, pp. 576–594.
[8] A. K. Saxena, P. Scivatava, R. K. Kale, N. Z. Baquer, *Biochem. Pharmacol.* **1993**, *45*, 539.
[9] X. Shan, T. Y. Aw, D. P. Jones, *Pharmacol. Ther.* **1990**, *47*, 61.
[10] S. H. Thomas, *Pharmacol. Ther.* **1993**, *60*, 91.
[11] G. M. Adamson, R. E. Billings, *Arch. Biochem. Biophys.* **1992**, *294*, 223.
[12] F. J. T. Staal, M. T. Anderson, G. E. J. Staal, L. A. Herzenberg, C. Gitler, L. Herzenberg, *Proc. Natl. Acad. Sci USA* **1994**, *91*, 3619.
[13] F. J. T. Staal, M. Roederer, L. A. Herzenberg, L. Herzenberg, *Proc. Natl. Acad. Sci. USA* **1990**, *87*, 9943.
[14] S. Mihm, J. Ennen, U. Pessara, R. Kurth, W. Droge, *AIDS* **1991**, *5*, 497.
[15] A. Fernadez, J. Kiefer, L. Fosdick, D. J. McConkey, *J. Immunol.* **1995**, *155*, 5133.
[16] L. A. Herzenberg, S. C. De Rosa, J. Gregson Dubs, M. Roederer, M. T. Anderson, S. W. Ela, S. C. Deresinski, L. A. Herzenberg, *Proc. Natl. Acad. Sci. USA* **1997**, *94*, 1967.
[17] N. D. Chasteen, *Struct. Bonding* **1983**, *53*, 105.
[18] a) M. Garner, J. Reglinski, W. E. Smith, J. McMurray, I. Abdullah, R. Wilson, *J. Biol. Inorg. Chem.* **1997**, *2*, 235; b) D. C. Crans, M. Mahroof-Tahir, A. D. Keramidas, *Mol. Cell. Biochem.* **1995**, *153*, 17.
[19] I. G. Macara, K. Kustin, L. C. Cantely, *Biochem. Biophys. Acta* **1980**, *629*, 95.
[20] T. V. Hansen, J. Aaseth, J. Alexander, *Arch. Toxicol.* **1982**, *50*, 195.
[21] K. A. Rubinson, *Proc. R. Soc. London Ser. B* **1981**, *212*, 65.
[22] H. Sakurai, S. Shimomura, K. Fukuzawa, K. Ishizu, *Biochem. Biophys. Res. Commun.* **1980**, *90*, 293.
[23] Z. Shi, Z. Sun, N. S. Dalal, *FEBS Lett.* **1990**, *271*, 185.
[24] H. Sakurai, S. Shimomura, K. Ishizu, *Inorg. Chim. Acta* **1981**, *55*, L67.
[25] E. G. Ferrer, P. A. M. Williams, E. J. Baran, *Biol. Trace Elem. Res.* **1991**, *30*, 175.
[26] E. G. Ferrer, P. A. M. Williams, E. J. Baran, *J. Inorg. Biochem.* **1993**, *50*, 253.
[27] A. Dessi, G. Micera, D. Sanna, *J. Inorg. Biochem.* **1993**, *52*, 275.
[28] H. Degani, M. Gochin, S. J. D. Karlish, Y. Shechter, *Biochemistry* **1981**, *20*, 5795.
[29] M. Delfini, E. Gaggeli, A. Lepri, G. Valensin, *Inorg. Chim. Acta* **1985**, *107*, 87.
[30] A. J. Tasiopoulos, A. T. Vlahos, A. D. Keramidas, T. A. Kabanos, Y. G. Deligiannakis, C. P. Raptopoulou, A. Terzis, *Angew. Chem.* **1996**, *108*, 2676; *Angew. Chem. Int. Ed. Engl.* **1996**, *35*, 2531.

[31] N. Baidya, M. M. Olmstead, P. M. Mascharak, *Inorg. Chem.* **1989**, 3426.

[32] A. D. Keramidas, A. B. Papaioannou, A. Vlahos, T. A. Kabanos, G. Bonas, A. Makriyannis, C. P. Raptopoulou, A. Terzis, *Inorg. Chem.* **1996**, *35*, 357.

[33] A. J.Tasiopoulos, Y. G. Deligiannakis, J. D. Woollins, A. M. Z. Slawin, T. A. Kabanos, *Chem. Commun.* **1998**, 569.

[34] a) W. Tsagkalidis, D. Rehder, *J. Biol. Inorg. Chem.* **1996**, *1*, 507; b) C. C. Cummins, R. R. Schrock, W. M. Davis, *Inorg. Chem.* **1994**, *33*, 1448; c) A. Sundheim, C. Theers, R. Matters, *Z. Naturforsch.* **1994**, *49b*, 176.

[35] H. Sakurai, Z. Jaira, N. Sakai, *Inorg. Chim. Acta* **1988**, *151*, 85.

[36] J. C. Dutton, G. D. Fallon, K. S. Murray, *Inorg. Chem.* **1988**, *27*, 34.

[37] T. B. Wen, J. C. Shi, X. Huang, Z. N. Chen, Q. T. Liu, B. S. Kang, *Polyhedron* **1998**, *17*, 331.

[38] P. R. Klich, A. T. Daniher, P. R. Challen, D. B. McConville, W. J. Youngs, *Inorg. Chem.* **1996**, *35*, 347.

[39] W. Tsagkalidis, D. Rodewald, D. Rehder, V. Vergopoulos, *Inorg. Chim. Acta* **1994**, *219*, 213.

[40] J. K. Money, J. C. Huffman, G. Christou, *Inorg. Chem.* **1984**, *24*, 3297.

[41] a) B. J. Hamstra, A. L. P. Houseman, G. J. Colpas, J. W. Kampt, R. Lobrutto, W. D. Frasch, V. L. Pecoraro, *Inorg. Chem.* **1997**, *36*, 4866; b) I. Cavaco, J. C. Pessoa, D. Costa, M. T. Duarte, R. D. Gillard, P. Matias, *J. Chem. Soc. Dalton Trans.* **1994**, 149.

[42] a) A. Neves, W. Walz, K. Wieghardt, B. Nuber, J. Weiss, *Inorg. Chem.* **1988**, *27*, 2484; b) K. Kanamori, I. Kazuhito, K. I. Okamoto, *Acta Crystallogr.* **1997**, *C53*, 672; K. Kanamori, K. Miyazaki, K. I. Okamoto, *Acta Crystallogr.* **1997**, *C53*, 673.

[43] J. Chakravarty, S. Dutta, S. K. Chandra, P. Basu, A. Chakravorty, *Inorg. Chem.* **1993**, *32*, 4249.

[44] S. G. Brand, N. Edelstein, C. J. Hawkins, G. Shalimoff, M. R. Snow, E. R. T. Tiekink, *Inorg. Chem.* **1990**, *29*, 434.

[45] M. A. A. F. de C. T. Carrondo, M. T. L. S. Duarte, J. A. L. Silva, J. J. R. Frausto da Silva, *Polyhedron* **1991**, *10*, 73.

[46] P. Basu, S. Pal, A. J. Chakravorty, *J. Chem. Soc. Dalton Trans.* **1991**, 3217.

[47] The V–Cl and V=O bond length in mononuclear octahedral compounds containing the unit *cis*-$V^{IV}OCl$ range form 2.295 to 2.400 and from 1.579 to 1.624 Å, respectively. a) H. Kelm, H. J. Kruger, *Inorg. Chem.* **1996**, *35*, 2533; b) T. A. Kabanos, A. D. Keramidas, A. Papaioannou, A. Terzis, *Inorg. Chem.* **1994**, *33*, 845; c) W. Priebsch, D. Rehder, *Inorg. Chem.* **1990**, *29*, 3013; d) G. R. Willey, M. T. Lakin, N. W. Alcock, *J. Chem. Soc. Chem. Commun.* **1991**, 1414; e) J. Zah-Letho, E. Samuel, Y. Dromzee, Y. Jeannin, *Inorg. Chim. Acta* **1987**, *126*, 35.

[48] C. J. Ballhausen, H. B. Gray, *Inorg. Chem.* **1962**, *1*, 111.

[49] R. S. Nicholson, I. Shain, *Anal. Chem.* **1964**, *36*, 706.

[50] K. Nakamoto, *Infrared and Raman Spectra of Inorganic and Coordination Compounds*, 4th ed., Wiley, New York, **1986**, pp. 227–244.

[51] G. B. Deacon, R. J. Phillips, *Coord. Chem. Rev.* **1980**, *33*, 227.

[52] N. D. Chasteen, in *Biological Magnetic Resonance*, *Vol. 3* (Eds.: L. Berliner, J. Reuben), Plenum, New York, **1981**, p. 53.

[53] H. Sakurai, J. Hirata, H. Michibata, *Biochem. Biophys. Res. Commun.* **1987**, *149*, 411.

[54] A. Jezierski, J. B. Raynor, *J. Chem. Soc. Dalton Trans.* **1981**, 1.

[55] S. G. Brand, MSc Thesis, University of Queensland, **1987.**

[56] J. C. Dutton, G. D. Fallon, K. S. Murray, *Inorg. Chem.* **1988**, *27*, 34.

[57] J. K. Money, K. Folting, J. C. Huffman, D. Collison, J. Temperley, F. E. Mabbs, G. Christou, *Inorg. Chem.* **1986**, *25*, 4583.

[58] T. B. Wen, J. C. Shi, X. Huang, Z. N. Chen, Q. T. Liu, B. S.Kang, *Polyhedron* **1998**, *17*, 331.

[59] B. McGarvey, in *Transition Metal Chemistry*, *Vol. 3* (Ed.: R. L. Carlin), Marcel Dekker, New York, **1996**, p. 89.

[60] B. A. Goodman, J. D. Raynor, *Adv. Inorg. Chem. Radiochem.* **1970**, *13*, 135.

[61] L. J. Boucher, E. C. Tynan, T. F. Yen, in *Electron Spin Resonance of Metal Complexes* (Ed.: T. F. Yen), Plenum, New York, **1969**, p. 111.

[62] C. M. Guzy, J. B. Raynor, M. C. R. Symons, *J. Chem. Soc. A* **1969**, 2791.

[63] C. R. Cornman, E. P. Zovinka, Y. D. Boyajian, K. M. Geiser-Bush, P. D. Boyle, P. Singh, *Inorg. Chem.* **1995**, *34*, 4213.

[64] G. R. Hanson, T. A. Kabanos, A. D. Keramidas, D. Mentzafos, A. Terzis, *Inorg. Chem.* **1992**, *31*, 2597.

[65] H. Sigel, R. B. Martin, *Chem. Rev.* **1982**, *82*, 385.

[66] F. C. Anson, T. J. Collins, S. L. Gibson, J. T. Keeth, T. E. Krafft, G. T. Peake, *J. Am. Chem. Soc.* **1986**, *108*, 6593 and references therein.

[67] P. V. Bernhardt, G. A. Lawrence, P. Comba, L. L. Martin, T. W. Hambely, *J. Chem. Soc. Dalton Trans.* **1990**, 2859.

[68] The EPR parameters for the $[VOCl_4]^{2-}$ reported here are slightly different from those previously reported for $[VOCl_4]^{2-}$, $g_{x,y} = 1.9979$, $g_z = 1.948$, $A_{x,y} = 62.8$ and $A_z = 168 \times 10^{-4}\,cm^{-1}$; J. M. Flowers, J. C. Hempel, W. E. Hatfield, H. H. Dearman, *J. Chem. Phys.* **1973**, *58*, 1479. We attribute this difference to the different solvation environment, i.e. frozen ethyl alcohol in our case vs. $NH_4[SbCl_6]$ matrix in Flowers et al.

[69] For the calculation of the $A_{z,amide}$ value of the oxovanadium(IV) compounds, **3**, **4** $\cdot$ 2 CH_3OH and **5** $\cdot$ CH_3OH, the A_z value for the phenanthroline nitrogen was required. The EPR spectrum of $[VOCl_2(CH_3OH)(phen)]$ (**7**) in various organic solvents consistently contained two spectra with intensity ratios close to 1:3, indicating the presence of two species in solution. The crystallographic data for **7** reveal that in the solid state, it exists only in a single conformation, in which both phenanthroline nitrogens are equatorially ligated to the $V^{IV}O^{2+}$ center. On the basis of the A_z and g_z values, we believe that the major component observed in the EPR spectrum of **7** corresponds to the conformation seen in Figure 2. The EPR parameters for the major EPR species of **7** are listed in Table 5.

[70] S. A. Dikanov, D. Y. Tgvetkov, *ESEEM Spectroscopy*, CRC, Boca Raton, New York, **1992**.

[71] G. J. Gerfen, P. M. Hanna, N. D. Chasteen, D. J. Singel, *J. Am. Chem. Soc.* **1991**, *113*, 9513.

[72] S. A. Dikanov, C. Burgard, J. Hüttermann, *Chem. Phys. Lett.* **1994**, *212*, 493.

[73] A. L. P. Houseman, L. Morgan, R. LoBrutto, W. D. Frasch, *Biochemistry* **1994**, *33*, 4910.

[74] Based on our ESEEM data the hyperfine coupling parameters are: $A(N_{amine}) = 4.8$ MHz, $A(N_{amide}) = 8.1$ MHz, $A(N_{phen}) = 5.1$ MHz.

[75] D. Rehder, C. Weidemann, A. Duch, W. Priebsch, *Inorg. Chem.* **1987**, *27*, 584.

[76] D. C. Crans, H. Holst, A. D. Keramidas, D. Rehder, *Inorg. Chem.* **1995**, *34*, 2524.

[77] D. C. Crans, P. K. Shin, *J. Am. Chem. Soc.* **1994**, *116*, 1305.

[78] F. W. B. Einstein, R. J. Batchelor, S. J. Angus-Dunne, A. S. Tracey, *Inorg. Chem.* **1996**, *35*, 1680.

[79] C. R. Cornman, K. M. Geiser-Bush, S. P. Rowley, P. D. Boyle, *Inorg. Chem.* **1997**, *36*, 6401.

[80] R. Chand-Paul, S. Bathia, A. Kuman, *Inorg. Synth.* **1982**, 181.

[81] R. G. Kern, *J. Inorg. Nucl. Chem.* **1962**, *24*, 1105.

[82] R. A. Rowe, M. M. Jones, *Inorg. Synth.* **1957**, *5*, 113.

[83] Abbreviations: CV, cyclic voltammetry; EPR, electron paramagnetic resonance; ESEEM, electron spin echo envelope modulation; $acac^-$, pentane-2,4-dionate; edt^{2-} ethane-1,2-dithiolate; $tsalphen^{2-}$, *N,N'-0*-phenylenebis(thiosalicylidene-aminate); $thipca^{2-}$, *N*-[2-(2-thiophenoylmethylene)aminophenyl]pyridine-2-carboxamidate; $Hmpp^-$, 2-mercapto-3-pyridinolate; bpy, 2,2′-bipyridine; phen, 1,10-phenanthroline; $salen^{2-}$, *N,N'*-ethylenebis(salicylideneaminate); $acacen^{2-}$, bis(acetylacetone)ethylenediiminate; $paap^{2-}$, 1,2-bis(2-pyridinecarboxamide)benzenate; $phepca^{2-}$, *N*-[2-(2-phenolylmethylene)amino]-pyridine-2-carboxamidate; $pycac^{2-}$, *N*-[2-(4-oxopent-2-en-2-ylamino)phenyl]pyridine-2-carboxamidate; $pycbac^{2-}$, *N*-[2-(4-phenyl-4-oxobut-2-en-2-ylamino)phenyl]pyridine-2-carboxamidate; $hypyb^{3-}$, 1-(2-hydroxybenzamido)-2-(2-pyridine-carboxamido)benzenate; $hymeb^{4-}$, 1,2-bis(2-hydroxy-2-methylpropanamid)benzenate; $hybeb^{4-}$, 1,2-bis(2-hydroxybenzamido)benzenate.

[84] D. Kivelson, S. K. Lee, *J. Chem. Phys.* **1964**, *41*, 1986.

[85] A. Hitchman, R. L. Belford, *Inorg. Chem.* **1969**, *8*, 958.

[86] I. Heyrovsky, D. Ilkovic, *Collect. Czech. Chem. Commun.* **1935**, *7*, 198.

[87] R. R. Gagne, C. A. Koral, G. C. Lisensky, *Inorg. Chem.* **1980**, *19*, 2854.

[88] H. M. Koepp, H. Wendt, H. Z. Strehlow, *Z. Elektrochem.* **1960**, *64*, 483.

[89] D. C. Crans, *Comments on Inorganic Chemistry* **1994**, 16, 1.

Received: June 18, 1998 [F1219]